Osmotic pressure and viscoelastic shear moduli of concentrated emulsions

T. G. Mason,[1] Martin-D. Lacasse,[2] Gary S. Grest,[2] Dov Levine,[3] J. Bibette,[4] and D. A. Weitz[5]
[1]*Department of Chemical Engineering, Johns Hopkins University, Baltimore, Maryland 21218*
[2]*Corporate Research Science Laboratories, Exxon Research and Engineering Company, Annandale, New Jersey 08801*
[3]*Department of Physics, Technion, Haifa, 32000 Israel*
[4]*Centre de Recherche Paul Pascal, Avenue Dr. A. Schweitzer, F-33600 Pessac, France*
[5]*Department of Physics and Astronomy, University of Pennsylvania, Philadelphia, Pennsylvania 19104*
(Received 24 February 1997)

We present an experimental study of the frequency ω dependence and volume fraction φ dependence of the complex shear modulus $G^*(\omega,\varphi)$ of monodisperse emulsions which have been concentrated by an osmotic pressure Π. At a given φ, the elastic storage modulus $G'(\omega)=\mathrm{Re}[G^*(\omega)]$ exhibits a low-frequency plateau G'_p, dominating the dissipative loss modulus $G''(\omega)=\mathrm{Im}[G^*(\omega)]$ which exhibits a minimum. Above a critical packing fraction φ_c, we find that both $\Pi(\varphi)$ and $G'_p(\varphi)$ increase quasilinearly, scaling as $(\varphi-\varphi_c)^\mu$, where $\varphi_c \approx \varphi_c^{\mathrm{rcp}}$, the volume fraction of a random close packing of spheres, and μ is an exponent close to unity. To explain this result, we develop a model of disordered droplets which interact through an effective repulsive anharmonic potential, based on results obtained for a compressed droplet. A simulation based on this model yields a calculated static shear modulus G and osmotic pressure Π that are in excellent agreement with the experimental values of G'_p and Π. [S1063-651X(97)15008-5]

PACS number(s): 82.70.Kj, 81.40.Jj, 62.20.Dc

I. INTRODUCTION

An emulsion is an immiscible mixture of two fluids, one of which is dispersed in the continuous phase of the other, typically made by rupturing droplets down to colloidal sizes through mixing. To inhibit recombination, or coalescence, a surfactant which concentrates at the interfaces must be added to create a short-ranged interfacial repulsion between the droplets [1,2]. For an appropriate surfactant, a quantity much less than the mass of the liquids is often sufficient to make this interfacial repulsion strong enough to render the emulsion kinetically stable against coalescence and demixing for many years. This kinetic stability differentiates emulsions from thermodynamically stable microemulsions which form spontaneously without mixing when the proper proportions of certain fluids and surfactants are placed in contact.

Despite being comprised solely of fluids, emulsions consisting of highly concentrated droplets can possess a striking shear rigidity that is characteristic of a solid. The nature of this elasticity is unusual; it exists only because the repulsive droplets have been compressed by an external osmotic pressure Π, and thus concentrated to a sufficiently large droplet volume fraction φ, which permits the storage of interfacial elastic shear energy. For instance, if $\Pi(\varphi)$ approaches the characteristic Laplace pressure required to deform the droplets $(2\sigma/R)$, where σ is the interfacial tension and R is the undeformed droplet radius, the droplets pack together and deform, creating flat facets where neighboring droplets touch. As the osmotic pressure is raised even further, φ tends toward unity, and the emulsion resembles a biliquid foam. Provided the droplets are compressed by an osmotic pressure, additional energy can be stored by imposing shear deformations which create additional droplet surface area; this gives rise to the emulsion's elastic modulus. However, if a concentrated emulsion is diluted, so that the osmotic pressure drops well below the Laplace scale, the resulting emulsion of unpacked spherical droplets loses it shear rigidity and is dominantly viscous, like the suspending fluid. Thus emulsions are versatile materials whose rheological properties can range from viscous to elastic depending on the applied osmotic pressure, and therefore φ. It is precisely this broad range of rheological behavior that gives rise to many technological applications; low viscosity oils can be made effectively rigid if emulsified in water and osmotically compressed to high volume fractions, while high viscosity oils can be made to flow more readily if emulsified at dilute volume fractions in water.

Emulsions possess microscopic mechanisms for both elastic energy storage and viscous dissipation. They are viscoelastic, exhibiting a stress response to a dynamically applied shear strain that is partially liquidlike and partially solidlike. The energy storage and dissipation per unit volume can be represented by the frequency-dependent complex viscoelastic shear modulus $G^*(\omega,\varphi)$, which is defined only for perturbative shears in which the stress and strain are linearly proportional [3,4]. The real part $G'(\omega)=\mathrm{Re}[G^*(\omega)]$, or storage modulus, is the in-phase ratio of the stress with respect to an oscillatory strain, and reflects elastic mechanisms, whereas the imaginary part $G''(\omega)=\mathrm{Im}[G^*(\omega)]$, or loss modulus, is the out-of-phase ratio of the stress with respect to the strain and reflects dissipative mechanisms. Linearity and causality imply that $G'(\omega)$ and $G''(\omega)$ are interrelated by the Kramers-Kronig relations [3–5] indicating their inherent link to the dissipation of shear stress and strain fluctuations in an emulsion. Understanding $G^*(\omega,\varphi)$ for well-controlled emulsions over a wide range of φ would provide valuable insight into the importance of the elastic and dissipative mechanisms as the droplets become packed and deformed.

In this paper, we present experimental measurements of the osmotic pressure and complex shear modulus of monodisperse emulsions compressed to different volume fractions.

By using well-controlled emulsions consisting of droplets of a single size [6,7], our approach offers several advantages over previous rheological experiments [8,9,19] which were made using emulsions having a broad distribution of droplet sizes. Indeed, polydisperse emulsions are difficult to study because they contain droplets with many different Laplace pressures so that, at a fixed osmotic pressure, the large droplets may deform significantly while the small droplets remain essentially undeformed. Moreover, the droplet packing and deformation cannot be easily connected to φ because small droplets can fit into the interstices of larger packed droplets. By contrast, using monodisperse emulsions eliminates these inherent difficulties: all the droplets have the same Laplace pressure. Moreover, the volume fraction can be simply related to the packing of identical spheres, thus allowing for meaningful comparisons with theoretical predictions which have usually assumed that the emulsion is monodisperse and ordered.

The earliest calculations of $\Pi(\varphi)$ and $G(\varphi)$ for emulsions and foams [11–17] are based on perfectly ordered crystals of droplets. In such systems at a given volume fraction and applied shear strain, all droplets are compressed equally and deform affinely under the shear; thus all droplets have exactly the same shape. Describing the dependence of Π and G on φ then reduces to the ''simpler'' problem of solving for the interfacial shape of a single droplet within a unit cell. Nevertheless, calculating the exact shape and area of such a single droplet at all $\varphi > \varphi_c$ is a very difficult free-boundary problem that can only be solved analytically for simple cases [16], or numerically [16,17]. Real emulsions, however, exhibit a disordered droplet structure, and a comparison of experimental results to these theoretical predictions is inappropriate. In particular, the comparison of the φ dependence of the low-frequency plateau value of the storage modulus of disordered, monodisperse emulsions to the static shear modulus predicted by these studies has demonstrated the existence of significant discrepancies [18].

The origin of the elasticity of an emulsion arises from the packing of the droplets; forces act upon each droplet due to its neighboring droplets pushing on it to withstand the osmotic pressure. However, all these forces must balance to maintain mechanical equilibrium. Calculations of the elastic properties of such disordered packings are complicated by the many different droplet shapes and the necessity of maintaining mechanical equilibrium as the droplets press against one another in differing amounts. While a general theory of the elasticity of disordered packings may ultimately lead to a precise analytical description of emulsion elasticity, computer simulations including adequate interdroplet interactions and accounting for the complexity associated with disorder can provide insight into the origins of the φ-dependent shear modulus. In order to understand the effects introduced by disorder, we developed a model for compressed emulsions which includes a disordered structure as well as realistic droplet deformations [10]. In this model, we formulate an anharmonic potential for the repulsion between the packed droplets, based on numerical results obtained for individual droplets when confined within regular cells [16]. Numerical results for the osmotic pressure Π and the static shear modulus G obtained from this model are in excellent agreement with our experimental values of Π and the elasticity, as can be shown from Fig. 1. We measure the frequency dependent storage modulus $G'(w,\varphi)$, and take the low-frequency plateau values $G'_p(\varphi)$ as the static shear modulus $G(\varphi)$. Our model of emulsions as disordered packings of repulsive elements is very general, and may also be applicable to other materials which become elastic under an applied osmotic compression, provided the potential between the elements is appropriately modified.

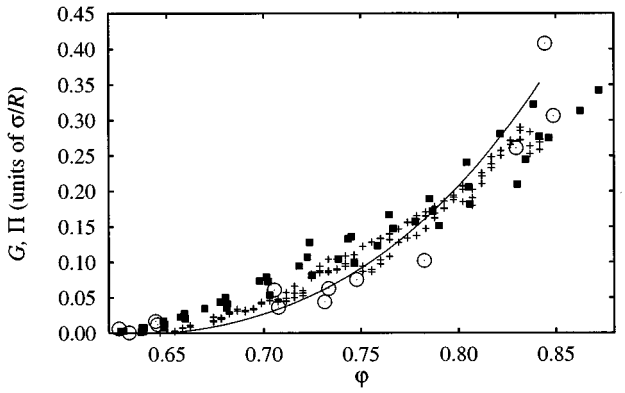

FIG. 1. The scaled shear modulus and osmotic pressure as a function of φ. The computed scaled static shear modulus $G/(\sigma/R)$ (+) and osmotic pressure $\Pi/(\sigma/R)$ (line), as obtained from the model presented in Sec. IV B 2, are compared with the experimental values of $G'_p(\varphi_{\rm eff})$ (■) and $\Pi(\varphi_{\rm eff})$ (○).

The structure of this paper is as follows. In Sec. II, we review the theoretical predictions for the osmotic pressure and shear rheology of emulsions. In Sec. III, the experimental aspects of this study are described; Sec. III A describes the emulsion preparation and the rheological measurement techniques; Sec. III B presents the results of our measurements; and Sec. III C compares our experimental observations to existing predictions and previous measurements. In order to understand the difference found between our results and the predictions existing for ordered arrays of droplets, in Sec. IV we present the results of numerical studies based on a model that can account for disorder. In Sec. IV A, we describe the details and the motivation of the model, while, in Sect. IV B we present and discuss the simulation results. A brief conclusion closes the paper.

II. THEORY

In order to understand the properties of packings of deformable spheres, it is useful first to review the packing of static, solid spheres. Their packing determines the critical volume fraction φ_c at which the onset of droplet deformation occurs and the coordination number z_c of nearest neighbors touching a given droplet. The highest volume fraction of monodisperse hard spheres is attained for ordered crystalline structures, including face-centered-cubic (fcc) and hexagonal close packing (hcp). These have $\varphi_c^{\rm cp} = \pi\sqrt{2}/6 \approx 0.74$ and $z_c^{\rm cp} = 12$. By randomly varying the stacking order of the planes, a random hexagonally close-packed (rhcp) structure can be made, but this does not alter either φ_c or z_c. Other ordered packings are less dense. For example, the body-centered-cubic (bcc) packing has $\varphi_c^{\rm bcc} = \pi\sqrt{3}/8 \approx 0.68$ and $z_c^{\rm bcc} = 8$, while the simple cubic (sc) packing has

$\varphi_c^{sc}=\pi/6\approx 0.52$ and $z_c^{sc}=6$. The strict definition of a packing excludes conditions of mechanical stability. However, under an interdroplet potential that is purely repulsive and spherically symmetric as the one found in emulsions, both bcc and sc are unstable against weak random mechanical agitations.

By contrast to ordered packings, mechanically stable disordered packings occur at significantly lower volume fractions. By shaking loosely packed macroscopic ball bearings [20], or through entropically driven Brownian motion for colloidal-sized particles, the packing density can be increased up to a reproducible limit termed random close packing (rcp) for which $\varphi_c^{rcp}\approx 0.64$ [21] (conjectured to be $2/\pi$ [22]) and at an average coordination number $\overline{z_c^{rcp}}\approx 6$ [10]. From experimental observation, this is the highest volume fraction at which disordered monodisperse hard spheres can be packed.

While increasing the volume fraction of a dilute colloidal system toward φ^{rcp}, the packing of spheres undergoes an ergodic to nonergodic transition, or a colloidal glass transition, at a value φ_g well below φ^{rcp}. Above φ_g, every sphere is confined into a local region by the cage formed by its neighbors; however, there remains some degree of local translational free volume within its cage. Despite this motion, the global configuration remains locked into a glassy structure, since the probability for a sphere to diffuse out of its cage over a reasonable time scale is essentially zero. Below φ_g, the system exhibits an ergodic behavior. The colloidal glass transition is well-described by mode-coupling theory (MCT), which assumes that the vibrational modes of the glassy structure at different wave vectors are inherently coupled [23]; it predicts that $\varphi_g\approx 0.58$. Light-scattering measurements [24] and mechanical rheological measurements [25] of disordered colloidal hard-sphere suspensions support this prediction for φ_g.

The behavior of an emulsion for $\varphi<\varphi_c$ is expected to be reminiscent of that of hard spheres; any elastic behavior is entropic in nature [25]. We emphasize, however, that the magnitude of this entropic elasticity is significantly lower than that controlled by surface tension, since $k_BT\ll\sigma R^2$; nevertheless, below φ_c it is measurable. As the volume fraction is increased further, one eventually reaches a volume fraction at which the droplets can no longer pack without deforming; for a disordered monodisperse emulsion, this occurs initially at $\varphi\sim\varphi_c^{rcp}$. Since the interactions between emulsion droplets are purely repulsive, work must be done against surface tension to compress and deform the droplets. This work is done through the application of an osmotic pressure and the resulting excess surface area of the droplets determines the equilibrium elastic energy stored at a fixed osmotic pressure. The additional excess surface area created by a perturbative shear deformation determines the static shear modulus $G(\varphi)$. Thus the elasticity and the osmotic pressure are both controlled by the surface tension of the droplets, or their Laplace pressure. Although Π and G represent fundamentally different properties, they both depend on the degree of droplet deformation and therefore φ. In principle, both can be determined if all the droplet shapes are known. These shapes depend upon the overall positional structure, or packing, of the droplets as they press against their neighbors in mechanical equilibrium, and also upon the detailed geometries of the individual contacts.

For an emulsion of oil in water stabilized by an ionic surfactant, each interdroplet contact is in reality a charged system of interfaces oil-surfactant-water-surfactant-oil, making the contact purely repulsive and thus stable against coalescence. The presence of a thin water layer between interacting droplets exists at all volume fractions, including φ near unity. The screened double-layer repulsion has a strength determined by the surface potential and a range characterized by the Debye length λ_D [26]. These depend on the interfacial concentration of the surfactant, the bulk ionic concentration in the aqueous continuous phase, and the temperature. Two droplets forced together will begin to deform before their interfaces actually touch due to the electrostatic repulsion; the droplet system minimizes its total free energy by reducing the energy due to electrostatic repulsion at the expense of creating some additional surface area by deforming the droplet interfaces. Thus, the droplets have an effective radius larger than their actual size, and consequently, they deform for φ below φ_c [27,28]. This electrostatic repulsion can be accounted for by using an effective volume fraction which incorporates a first-order correction for the film thickness h,

$$\varphi_{\text{eff}}\approx\varphi[1+3/2(h/R)], \tag{1}$$

for $h\ll R$ [27]; this φ_{eff} represents the actual phase volume fraction of packing, allowing us to account exclusively for the effects of the packing. Although this approximation assumes that the droplets are spherical, it is valid to within 10% even for nearly polyhedral droplets near $\varphi\approx 1$ [29].

A. Osmotic pressure

Just as the structure and interactions between atoms determine the pressure-volume equation of state for homogeneous solids, the structure and interactions (deformability) between droplets determines the osmotic equation of state $\Pi(\varphi)$ of dispersions of droplets. The osmotic equation of state for emulsions governs the (osmotic) compression of the droplets at fixed total droplet volume, allowing the free exchange of solvent with a reservoir [30]. As the droplets are compressed by the osmotic pressure, their total surface area $A(\varphi)$ increases above that of the undeformed droplets A_o, which is, for example, $4\pi NR^2$ for a monodisperse collection of N droplets of undeformed radius R. For any monodisperse emulsion in d dimensions, the osmotic pressure is obtained from

$$\Pi(\varphi)/(\sigma/R)=d\varphi^2\,\frac{\partial}{\partial\varphi}\left[\frac{A(\varphi)}{A_o}\right]. \tag{2}$$

In this equation and what follows, we assume that the surface tension is constant. Below φ_c, the droplets are not compressed, so $A(\varphi)$ is constant ($A=A_o$) and any surface tension contribution to Π vanishes (an entropic contribution remains). By contrast, when the droplets are compressed above φ_c, their surface area increases as they press against neighboring droplets and deform, and Π increases.

The droplet response to compression has three characteristic regimes in three dimensions [16]. First, when the drop-

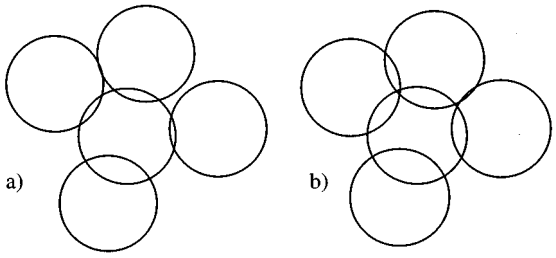

FIG. 2. Schematic representation of a uniform compression of a disordered cluster of droplets. In the initial state (a), the droplets are compressed to $\varphi > \varphi_c$ and are in mechanical equilibrium (surrounding droplets are not shown). The overlap of the circles is meant to indicate the degree of compression schematically, and the central force between each pair of droplets is some function of the overlap. In (b), the compression has been increased uniformly. Only for a Hookian force will the cluster remain in mechanical equilibrium.

lets are infinitesimally deformed, the interaction energy U between two droplets resulting from the increase of surface area is [13,16]

$$U(f)/(\sigma A_o) \sim \left(\frac{fR}{\sigma A_o}\right)^2 \left[a - \ln\left(\frac{fR}{\sigma A_o}\right)\right], \tag{3}$$

where f is the interdroplet force and a is a dimensionless constant. The range of validity of this expression is rather narrow, just after contact, and this behavior is significant only at the onset of the response of ordered emulsions. In terms of interdroplet distance, to first order, this potential can be shown [10] to be equivalent to $U(\xi) \sim -\xi^2/\ln\xi$.

The second regime of the droplet elastic response spans the much broader range of deformation that follows contact, and is therefore the most important when considering the response of real (disordered) emulsions. In this regime, the response of the droplets is *anharmonic*, with a behavior that can be approximated by a power law, where the power depends on the coordination number [10,16]. The anharmonicity of the potential has profound consequences on the deformations: even under a uniform compression, it implies that there are nonaffine particle displacements. To illustrate this, consider a *disordered* system of monodisperse spherical objects interacting with repulsive forces only, and compress the system uniformly at some $\varphi > \varphi_c^{\mathrm{rcp}}$. If the system is in mechanical equilibrium, any droplet i with z_i neighbors will have z_i forces $\mathbf{f}_{ij}$, $j = 1, \ldots, z_i$ acting on it and such that $\Sigma_j \mathbf{f}_{ij} = \mathbf{0}$. Now increase the compression uniformly, which amounts to reducing the interdroplet distances r_{ij} between centers of droplet i and j by a constant factor $\lambda < 1$, as pictured in Fig. 2. For a Hookian force, $\mathbf{f}_{ij}(\lambda \mathbf{r}_{ij}) = \lambda \mathbf{f}_{ij}(\mathbf{r}_{ij})$, and thus mechanical equilibrium remains after the transformation. For any other force, the droplet must move in different amounts so as to achieve a new equilibrium state. Thus, even for a relatively benign case of uniform compression, a nonharmonic force will lead to nonaffine motion of the constituent particles. Here we implicitly assumed that the number of contacts before and after compression is the same, an assumption that is clearly not true for a disordered system. Thus systems with a Hookian interdroplet potential are very likely not to respond affinely, since the creation of any new contact will change the conditions for local mechanical equilibrium.

This anharmonic region is followed by a third regime, in which the droplet response to compression sharply rises, due to volume conservation effects. This is the regime near the biliquid foam limit where $\varphi \to 1$, so that most of the continuous-phase liquid has been extracted; there only remains thin veins for which the radii of curvature of the free surfaces are very small, reflecting large Laplace pressures [19].

To capture the essential predictions for the osmotic equation of state of an ordered emulsion, we first consider the response of an array of droplets to a uniform compression near contact, i.e., at $\varphi \gtrsim \varphi_c$. For this purpose, we introduce a dimensionless displacement ξ defined by

$$\xi = 1 - (\varphi_c/\varphi)^{1/d}. \tag{4}$$

For an ordered array in d dimensions uniformly compressed at $\varphi > \varphi_c$, ξ is the dimensionless ratio of the perpendicular displacement of the facet toward the droplet center to the undeformed radius R. To obtain a rough estimate of $\Pi(\varphi)$, we make the following assumptions: the compression is assumed to be affine and the logarithmic term of Eq. (3) is ignored. Thus, for $\varphi \gtrsim \varphi_c$, $(\varphi - \varphi_c) \sim \xi$, and hence the energy can be approximated by $U(\varphi)/(\sigma A_o) \sim (\varphi - \varphi_c)^2$, reflecting a Hookian spring force, $f/(\sigma R) \sim \xi$. Using Eq. (2), one finds that the osmotic pressure in the weak compression limit is

$$\Pi(\varphi)/(\sigma/R) = B\varphi^2(\varphi - \varphi_c), \tag{5}$$

where both constants B and φ_c depend on the geometry of the droplet packing. Since φ^2 varies little in the vicinity of φ_c, the dominant scaling of Π is linear with respect to the difference of φ above packing.

Since the derivation of Eq. (5) relies on the assumptions of affinity and harmonicity, which are true for two-dimensional (2D) systems but are false for real (3D) disordered emulsions, it is not surprising to realize the similarity between this linear scaling form and that of Princen [11,12] who derived it for an ordered 2D monodisperse system of deformable circles of constant area. When the logarithmic corrections are included in the derivation of $\Pi(\varphi)$ for 3D systems [13], the linear form of Eq. (5) is still dominant.

Equation (3) is only valid at infinitesimal compression; it is thus appropriate to consider a more representative interdroplet potential. In fact, Eq. (5) can be shown to be a special case of a more general approach (see the Appendix): if the response of the droplets is assumed to be a power law $U(\xi) \sim [(1-\xi)^{-3} - 1]^{\alpha}$ [16], then the osmotic pressure obeys

$$\Pi(\varphi)/(\sigma/R) \sim \varphi^2(\varphi - \varphi_c)^{\alpha - 1}. \tag{6}$$

Since $\alpha \gtrsim 2$ for real droplets moderately compressed by six neighbors, Eq. (5) is somewhat recovered.

B. Static shear modulus

Similarly to the osmotic pressure, the static shear modulus $G(\varphi)$ is determined by the additional deformation of the

droplets away from their equilibrium shapes due to a perturbative static strain [31]. Princen [11] analyzed an ordered (monodisperse) 2D array of deformable circles and showed that $G=0$ for $\varphi<\varphi_c$, and then discontinuously jumps to nearly the Laplace pressure at φ_c, reflecting the elasticity of the circles themselves. The existence of an exact solution in two dimensions is possible because the droplet surface (more exactly the perimeter) is parametrized by only one radius of curvature, and therefore the minimum free surface is always an arc of a circle. Three-dimensional problems are much more elaborate. However, using the potential of Eq. (3) and uniaxially straining an emulsion with a sc packing, Buzza and Cates predicted a sharp but continuous rise of the uniaxial static shear modulus $G(\varphi)$ at φ_c [14]. This behavior arises because of the logarithmic divergence in the droplet response at small compression: as two droplets begin to touch ($\xi=0$), the effective spring constant f/ξ increases continuously but very sharply (divergent derivative) from zero to a finite value. As a result, the static shear modulus G of *ordered* emulsions does not exhibit a discontinuity at φ_c, as it would for a harmonic potential, but rather shows a very sharp but continuous rise [14,16]. It is not clear however, that the characteristic onset [cf. Eq. (3)] of the force at infinitesimal compression is determinant in the φ dependence of the static shear modulus for *disordered* emulsions at $\varphi>\varphi_c$. Indeed, while a quasilinear scaling of Π similar to Eq. (5) was measured experimentally for polydisperse (disordered) emulsions [19] (for which it was assumed that $\varphi_c\approx 0.71$), as well as for monodisperse emulsions [18] (for which $\varphi_c\approx\varphi_c^{\mathrm{rcp}}$), no sharp rise in $G(\varphi)$ was observed; rather, for both cases, a smooth increase of $G(\varphi)$ was observed at the same φ_c [8,18].

At this point, we have the following picture: the theoretical predictions for the static shear modulus of *ordered* monodisperse emulsions are that $G(\varphi)$ should exhibit a sharp rise (most likely continuous) at φ_c and then continue to increase with $d^2G/d\varphi^2\lesssim 0$; by contrast, existing experimental data for *disordered* monodisperse emulsions [18], which are displayed in Fig. 1, show that the static shear modulus $G(\varphi)$ increases smoothly at φ_c (with $(dG/d\varphi)|_{\varphi_c}\approx 0$), followed by a region of slight positive curvature ($d^2G/d\varphi^2>0$).

To reconcile this difference, the effect of disorder and the interdroplet potential must be taken into account. The behavior of $G(\varphi)$ near φ_c has been investigated in simulations, which unfortunately have been restricted to two dimensions, with disorder introduced through polydispersity [32–35]. These simulations find a jump of the static shear modulus at φ_c and a negative second derivative. We shall investigate these issues in more detail below.

Under strong compression, for which $\varphi\approx 1$ and the highly deformed droplets are nearly polyhedral, the use of the undeformed droplet radius to characterize the Laplace pressure is inadequate. Instead, the Laplace pressure must be obtained from the curvatures at a point on the nonspherical droplet free interface, i.e., $\sigma(R_1^{-1}+R_2^{-1})$, where the R_i's represent the local radii of curvature. One or both these radii can become vanishingly small at the free edges and Plateau borders [7]. This implies that the osmotic pressure needed to remove all the water to create perfectly polyhedral droplets with sharp edges becomes very large, and that the slope of the surface area $A(\varphi)$ diverges as φ approaches unity, regardless of the emulsion's packing structure. For 2D systems, for example, the osmotic pressure is expected to diverge as $\Pi(\varphi)/(\sigma/R)\sim(1-\varphi)^{-1/2}$ [12,34]. By contrast, the static shear modulus clearly does not diverge in the same limit. Assuming that the emulsion can be treated as a biliquid foam, two conditions for mechanical equilibrium must be imposed, namely, that the films meet at equal angles of 120°, and that only four edges can meet at equal tetrahedral angles. For a random 3D isotropic system of flat interfaces, theoretical work suggests that $G(1)/(\sigma/R)\approx 0.55$ at $\varphi\approx 1$ [36]. Princen's measurements [8,19] of polydisperse emulsions qualitatively support these predictions; he reported a divergence of Π and $G(1)/(\sigma/R)\approx 0.5$.

C. Viscoelastic response

While much attention has been given to the static shear modulus, emulsions are in fact viscoelastic. Thus the shear modulus is in reality a function of frequency. Moreover, in addition to a storage, or elastic modulus, they also possess a loss, or viscous modulus. The loss modulus is typically significantly less than the storage modulus for most compressed emulsions, and, as such, has received relatively little attention. The effective viscosity η_{eff} of a highly compressed emulsion under low frequency shear of infinitesimal amplitude was predicted by Buzza, Lu, and Cates [15]. Within this theory, the contribution to the viscosity due to capillary flow of the water through the thin films between the droplets is $(R/h)\,\eta_w$, where η_w is the water viscosity, and the contribution from the surface dilational viscosity of the surfactant monolayer κ_B, as more surface area is created, is κ_B/R:

$$\eta_{\mathrm{eff}}=\eta_w\,\frac{R}{h}+\frac{\kappa_B}{R}. \tag{7}$$

Using $\kappa_B\approx 10^{-2}$ P cm, this suggests that the dilational contribution dominates with $\eta_{\mathrm{eff}}\approx 10^4\,\eta_w$ for micrometer-sized droplets with $h\gtrsim 1$ nm. Regardless of the dissipative mechanism or packing structure, this theory implies that the low-frequency behavior of the loss modulus for concentrated emulsions varies linearly with frequency as $G''(\omega)\sim\eta_{\mathrm{eff}}\omega$. However, the magnitude of the prefactor predicted theoretically is significantly smaller than that measured experimentally. A possible origin for this anomalous viscous loss for disordered concentrated emulsions was suggested by Liu *et al.* [37]. Their approach allowed for some local, randomly distributed weak regions (faults) within the packing having a zero shear modulus in one plane. By averaging over the random orientations of these planes, an anomalously large contribution to the loss modulus was found, with an unusual frequency dependence, $G''(\omega)\sim\omega^{1/2}$. Due to the Kramers-Kronig relations, a similar power law must contribute to $G'(\omega)$. Both contributions were observed using a light-scattering technique for measuring the high-frequency viscoelastic moduli of emulsions [38].

At volume fractions well below φ_c, emulsion droplets can deform only slightly during momentary collisions with neighbors as they undergo Brownian motion. Thus, at these volume fractions, an emulsion's osmotic pressure and rheo-

logical properties should resemble those of hard-sphere suspensions. Since the free volume available for translation V_f of each sphere vanishes as $\varphi \rightarrow \varphi_c$, the entropic energy density, proportional to $k_B T/V_f$, should diverge for hard spheres. This sets the scale for $\Pi(\varphi)$ and $G'(\omega,\varphi)$, which should also diverge for hard spheres. For emulsions however, a divergence at φ_c is precluded by the possibility of deformation of the droplets. Such entropic contributions arising from the effects of excluded volume have not been incorporated into previous theories of Π and G' for concentrated emulsions of colloidal droplets. Instead, these theories have assumed that the droplets are sufficiently large that entropic contributions to the free energy can be neglected, forcing Π and G' to be zero below φ_c and purely interfacial in origin above φ_c. A complete theory for the viscoelasticity of emulsions must account for the crossover from the entropically dominated regime below φ_c to the interfacially dominated regime above φ_c.

To address this behavior at a heuristic level, a model for $G'(\omega,\varphi)$ and $G''(\omega,\varphi)$ for concentrated emulsions near φ_c has been proposed [25], by analogy with a similar model for concentrated suspensions of hard spheres near the colloidal glass transition. As with hard spheres, we assume that emulsion droplets form a colloidal glass when concentrated to the glass transition volume fraction φ_g, although we allow for the possibility that the deformability of the droplets may slightly alter the observed value of φ_g compared to that of hard spheres. Below φ_g, on the liquid side of the glass transition, MCT makes quantitative predictions for the asymptotic behavior of the temporal (droplet) density autocorrelation function which exhibits the β-relaxation plateau [39]. A universal feature of MCT below φ_g is that the autocorrelation function of any microscopic variable coupled to density fluctuations has the same generic form in the β-relaxation regime, and, therefore, the form for the stress autocorrelation function is predicted to be the same [23]. The glassy contribution to the viscoelastic moduli at low frequencies can be obtained by Fourier transforming the stress autocorrelation function into the frequency domain, while respecting the Kramers-Kronig relations; the magnitude of $G^*(\omega,\varphi)$ is set by the thermodynamic derivative of the stress with respect to strain. Below φ_g, the generic MCT form for the density autocorrelation function leads to a frequency plateau in $G'(\omega,\varphi)$ which reflects entirely entropic energy storage, and a frequency minimum in $G''(\omega,\varphi)$, which reflects rearrangements of the spheres at low ω and internal cage motion at high ω. Above φ_g, the frequency plateau in $G'(\omega,\varphi)$ persists, but the rise in $G''(\omega,\varphi)$ toward low ω disappears as the structural frustration associated with nonergodicity prevents colloidal relaxations of the hard spheres. At higher frequencies, contributions to both G' and G'' proportional to $\omega^{1/2}$ arise from a diffusional boundary layer between the spheres [40,41], and the φ-dependent solvent viscosity [42] contribution to G' proportional to ω. The rheological model superposes the low-frequency MCT and high-frequency contributions to the moduli; this implicitly assumes a wide separation of time scales between each of these processes. This model has provided a successful interpretation of the measured frequency dependencies of the viscoelastic moduli for hard spheres, which include a plateau in $G'(\omega)$ and minimum in $G''(\omega)$ [25], and it may also serve as a basis for understanding the moduli of emulsions when the droplets are not strongly compressed.

III. EXPERIMENT

A. Methodology

To make model monodisperse emulsions suitable for our study, crude polydisperse emulsions of polydimethylsiloxane (PDMS) silicone oil droplets in water are fractionated using a procedure based on a droplet-size-dependent depletion attraction [6]. The surfactant is sodium dodecylsulfate (SDS) at a concentration of $C = 10$ mM, only slightly above the critical micelle concentration, making micelle-induced depletion attractions negligible [6], yet sufficiently large to guarantee good interfacial stability [43]. Our own observations with optical microscopy have confirmed that the droplets are stable against coalescence at all φ studied. We have measured the surface tension of the SDS solution in contact with silicone oil and find $\sigma = 9.8$ dyn/cm using a duNouy ring method. Our emulsions have a polydispersity that has been measured to be about 10% of the radius using angle-dependent dynamic light scattering from a dilute emulsion [7]. Light-scattering measurements of the angle-dependent intensity from concentrated emulsions with $\varphi > 0.6$ confirm that the droplet structure factor resembles that of a disordered glass; at lower φ, a liquidlike structure has been observed [7]. All measurements have been made at room temperature.

We determine the osmotic equation of state $\Pi(\varphi)$, for an emulsion having $R = 0.48$ μm by first setting the osmotic pressure to concentrate a dilute emulsion, waiting for equilibration of φ, and then measuring φ by weighing the emulsion before and after the water has been evaporated. To set Π over a large dynamic range, we use three different techniques in order of decreasing compression: polymer dialysis in which a hydrophilic polymer withdraws water from between the droplets thereby deforming them; centrifugation in which the density difference between the oil and water in the presence of an effective gravity is used to concentrate an initially uniform dispersion of droplets into a cream; and simple creaming in the much lower gravitational field of the earth.

In the polymer dialysis technique [44], a dilute emulsion is enclosed in a semipermeable cellulose bag and immersed in a reservoir of strongly hydrophilic dextran solution having a known osmotic pressure that increases with polymer content. The cellulose bag has a pore size which is much smaller than the droplet radii and radii of gyration of the polymer, so only water and SDS can be freely exchanged between the polymer solution and the emulsion. To prevent destabilization of the droplet interfaces by a loss of SDS from the emulsion, the SDS concentration in the polymer solution is also fixed at 10 mM. The polymer's affinity for water drives water out of the emulsion, thereby raising φ. The measured volume fraction remains constant after two weeks of equilibration; this implies that the emulsion's Π has been set to that of the polymer solution. We repeat this procedure at several different polymer concentrations to apply different Π.

Due to imprecision of the dialysis calibration for $\Pi < 10^4$ dyn/cm^2, we use centrifugation at different speeds to set Π at these lower values. We centrifuge a known

amount of dilute emulsion, and then determine φ by skimming a small amount of the creamed emulsion off the top of the column and evaporating the water. After creaming, if all the droplets occupy a distance much less than that of the centrifuge's lever arm, the spatial gradient in the acceleration g can be neglected, and the osmotic pressure at the top can be determined: $\Pi = \ell \Delta\rho g \varphi_i$, where ℓ is the column height, φ_i is the initial volume fraction before centrifugation, and $\Delta\rho$ is the density mismatch between the oil droplets and water. This maximum osmotic pressure reflects the buoyant stress of all droplets below the exposed layer, independent of the spatial gradient in φ, since the total volume of droplets is known. For large Π, equilibration of φ typically takes several hours to one day. As the speed of the centrifuge is lowered to obtain very small Π, the equilibration time becomes many days, making centrifugation impractical. Thus, to achieve the lowest Π, we have allowed an emulsion to cream in the earth's gravity, and after an equilibration time of half a year, we have measured φ of the skimmed cream.

To investigate the dependence of the linear viscoelastic moduli on the droplet size, we measure $G'(\omega)$ and $G''(\omega)$ for four silicone oil-in-water emulsions having radii of $R = 0.25$, 0.37, 0.53, and 0.74 μm using a mechanical controlled-strain rheometer [45]. To set C and φ simultaneously, we first wash the purified emulsion with a SDS solution at $C = 10$ mM, and then we concentrate it to nearly $\varphi \approx 1$ by centrifugation. This highest φ is measured by evaporation of a sample removed from this reservoir. Lower φ are set by diluting samples with a 10-mM SDS solution to the total volume required by the rheometer geometry. All emulsions have been made with PDMS (viscosity $\eta_o = 12$ cP), except for the emulsion with $R = 0.53$ μm made with polyphenylmethylsiloxane (PPMS, $\eta_o = 235$ cP).

In order to measure $G^*(\omega,\varphi)$ at high volume fractions, we employ a cone and plate geometry, while for $\varphi \leqslant 0.60$, we use a double-wall Couette geometry with a larger surface area to increase the rheometer's stress sensitivity. Vigorous preshearing along an applied strain can reduce the measured stress as a result of emulsion fracturing, especially at high φ. Thus our measurements are performed directly after loading the sample. During loading, all emulsions are necessarily presheared perpendicular to the direction of the azimuthally applied strain as the two rheometer surfaces are moved into position; this preshear is radial for the cone and plate geometry, and axial for the double wall Couette geometry. A motor actuates a sinusoidal strain of amplitude γ at a frequency ω, and the magnitude of the stress $\tau(\omega)$, as well as its phase lag relative to the strain $\delta(\omega)$, are detected by a torque transducer. In the linear regime at small strains, the stress is also sinusoidal, and the storage modulus is $G'(\omega) = [\tau(\omega)\cos(\delta(\omega))]/\gamma$, while the loss modulus is $G''(\omega) = [\tau(\omega)\sin(\delta(\omega))]/\gamma$ [3]. By measuring the moduli of an emulsion using both geometries, we verified that the results are reproducible and independent of the geometry. We enclose the emulsion with a water-filled vapor trap to prevent any evaporation that may change φ; this can cause the elasticity of the emulsion to initially grow with time as it develops a skin layer having higher φ. Standing waves in the gap of either geometry are negligible over the range of frequencies and elasticities we probe.

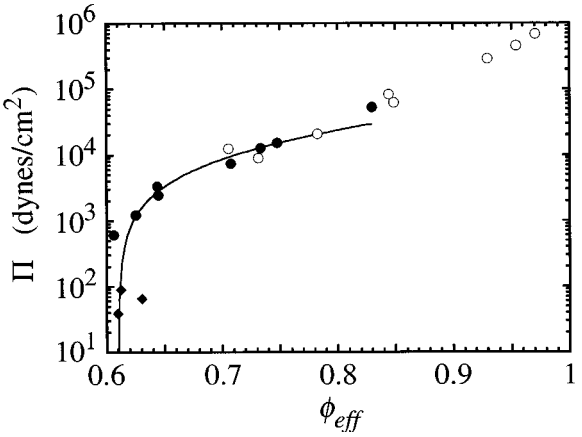

FIG. 3. The osmotic equation of state Π as a function of effective volume fraction, $\varphi_{\rm eff}$, of a monodisperse emulsion having radius $R = 0.48$ μm measured using dextran dialysis (○), centrifugation (●), and creaming in the earth's gravitational field (solid diamonds). The solid line is a fit to $\Pi(\varphi_{\rm eff})$ using the nearly linear weak compression prediction of the single droplet model in Eq. (5) for $\varphi_{\rm eff} \leqslant 0.80$. The effective volume fraction accounts for the thin films of water and is only slightly different than the oil volume fraction φ (see text).

Some previous measurements of the elastic moduli of emulsions employed a geometry in which slip was purposely induced at the walls of the cell, necessitating a complex correction for its effects to ensure that the proper moduli were determined [8,9]. We follow a different procedure, and ensure that no slip whatsoever occurs along the rheometer walls. We roughen the metal walls of the cells to a length scale somewhat larger than the droplet diameter; this eliminates wall slip [46]. We sandblasted the cone and plate, creating a roughness depth ranging from about 5 to 500 μm, larger than the micrometer-sized droplets. We verified that the measured $G'(\omega)$ and $G''(\omega)$ are the same for larger roughnesses introduced by milling regular grooves of 100 μm or 1 mm in the surfaces. The absence of slip has also been confirmed by varying the gap between the surfaces, and verifying that the measured moduli do not depend on the gap thickness.

B. Experimental results

The osmotic equation of state for an emulsion with $R = 0.48$ μm measured using polymer dialysis (open circles), centrifugation (solid circles), and ordinary creaming (diamonds) is shown in Fig. 3. Near $\varphi_{\rm eff} \approx 0.6 \approx \varphi_c^{\rm rcp}$, the osmotic pressure rises sharply, by several orders of magnitude, although the exact nature of this rise is obscured by experimental uncertainty in the measurement of φ, which is accurate to approximately 2%. Good agreement between the centrifugation and dialysis methods can be seen as $\Pi(\varphi)$ continues to rise, albeit less rapidly, well above φ_c. Near $\varphi_{\rm eff} \approx 1$, the osmotic pressure begins to rise more sharply again, reflecting the resistance of the droplets against assuming polyhedral shapes with small radii of curvature near their edges. For such extreme osmotic compressions, the water films can rupture allowing droplets to fuse, making the emulsion unstable, and the onset of droplet coalescence limits the highest φ we are able to explore.

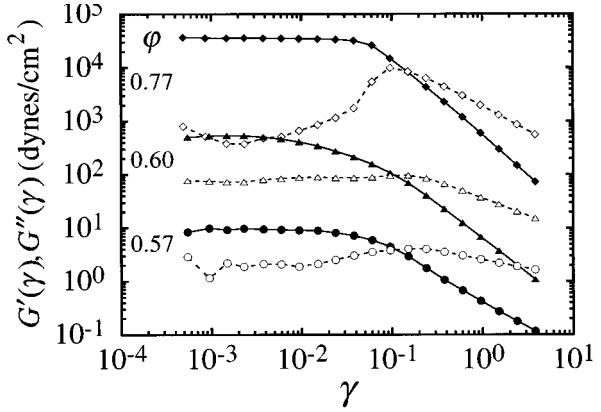

FIG. 4. The γ dependence of the storage, G', (solid symbols) and loss, G'' (open symbols) moduli of a monodisperse emulsion with $R \approx 0.53$ μm, for effective volume fractions of $\varphi_{\text{eff}} \approx 0.77$ ($\diamond$), 0.60 ($\triangle$), and 0.57 ($\bigcirc$), measured at $\omega = 1$ rad/s.

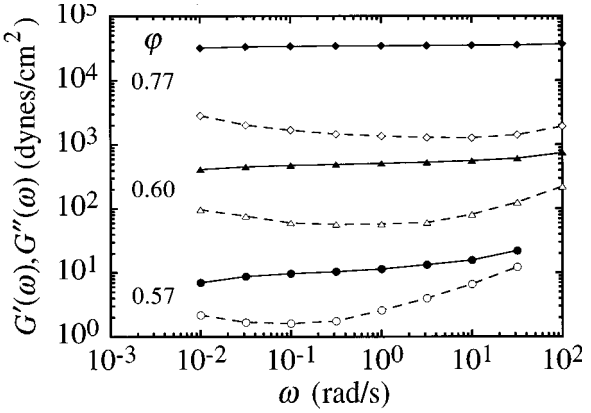

FIG. 5. The frequency dependence of the storage, G', (solid symbols) and loss, G'' (open symbols) moduli of a monodisperse emulsion with $R \approx 0.53$ μm, for $\varphi_{\text{eff}} = 0.77$ ($\diamond$), 0.60 ($\triangle$), and 0.57 ($\bigcirc$). The results for the two larger φ_{eff} were obtained with $\gamma = 0.005$, while those for the lowest were obtained with $\gamma = 0.015$.

To measure $G^*(\omega)$, we first establish the strain regime where the emulsion's stress response is linear. We set the frequency of the applied strain to $\omega = 1$ rad/s and sweep from small to large strain amplitudes to determine the extent of the linear regime. The measured linearity of $G^*(\omega)$ is not noticeably influenced by ω, although its asymptotic magnitude as $\gamma \to 0$ may vary with ω. The strain dependencies of $G'(\gamma, \varphi)$ and $G''(\gamma, \varphi)$ for a series of volume fractions are shown in Fig. 4 for $R = 0.53$ μm and $\omega = 1$ rad/s. The moduli are independent of strain below $\gamma \approx 0.02$ for the two lowest φ, showing that the linear regime exists only at very small strains. For these low strain values, $G'(\gamma)$ is greater than $G''(\gamma)$, reflecting the emulsion's dominantly elastic nature. At larger strains however, there is a slight but gradual drop in the storage modulus while the loss modulus begins to rise noticeably, indicating the approach to nonlinear yielding behavior and plastic flow. At very large strains, beyond the yield strain marked by the onset of the drop in $G'(\gamma)$, we observe that the temporal stress wave form is not sinusoidal, but becomes flattened at the peaks [47]. Since this response is nonlinear, G' and G'' are not strictly defined here; they are only apparent properties which reflect the peak stress to strain ratio and the phase lag defined by the temporal zero crossing of the stress relative to the strain. At these high values of strain, the apparent G'' dominates the apparent G', reflecting the dominance of energy loss introduced by the nonlinear flow.

To explore the time scales for stress relaxation, we fix a small strain amplitude which lies within the linear regime where G' and G'' are independent of γ, and measure $G^*(\omega)$ as a function of frequency. Using this very low value of peak strain ensures that our spectra reflect the emulsion's true linear moduli and are not influenced by increased dissipation typical at larger γ, in the nonlinear regime. By sweeping ω from high to low, we obtain $G'(\omega, \varphi)$ and $G''(\omega, \varphi)$; these are shown in Fig. 5. At all φ, we observe a low-frequency regime in which $G'(\omega)$ is constant or depends slightly on frequency. At the highest φ, $G'(\omega)$ is essentially independent of ω. At the lowest φ however, a plateau is still observed, but over a narrower frequency range, with $G'(\omega)$ dropping at low frequencies and rising at high frequencies. The low-frequency drop presumably reflects the very slow relaxation of the glassy structure of the emulsion, while the high-frequency rise reflects the fact that the system is comprised solely of fluids, whose viscous behavior dominates at sufficiently high frequencies. In order to define an equivalent to the static shear modulus, we define the plateau value $G'_p(\varphi)$ of the storage shear modulus $G'(\omega, \varphi)$; this is well defined at high volume fractions, while at lower φ, it is defined by the inflection point in $G'(\omega)$. In both cases, it reflects the overall magnitude of the static shear modulus $G(\varphi)$. The measured low-frequency plateau modulus increases over three decades from low to high φ.

By contrast to the plateau behavior of the dominant storage modulus $G'(\omega)$, the smaller loss modulus $G''(\omega)$ exhibits a minimum at frequencies close to the inflection point in $G'(\omega)$. The magnitude of this minimum, $G''_m(\varphi)$, also increases over three decades from lowest to highest φ. The minimum is shallow at the highest φ, but becomes more pronounced at lower φ.

We investigate how the droplet size influences $G'_p(\varphi)$ by examining emulsions having radii $R = 0.25$, 0.37, 0.53, and 0.74 μm. For $\varphi \leqslant 0.52$, the loss modulus dominates the storage modulus, and therefore $G'_p(\varphi)$ or $G''_m(\varphi)$ cannot be de-

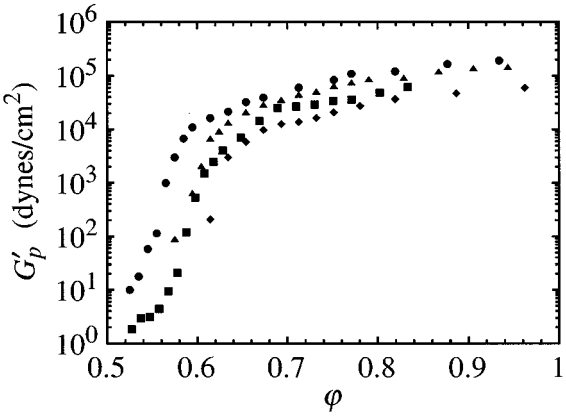

FIG. 6. The plateau storage modulus G'_p as a function of volume fraction for monodisperse emulsions having radii $R = 0.25$ μm (●), 0.37 μm ($\triangle$), 0.53 μm (■), and 0.74 μm ($\diamond$).

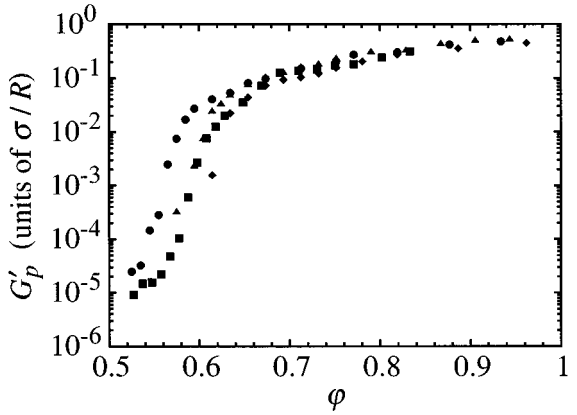

FIG. 7. The volume fraction dependence of the plateau storage modulus $G_p'(\varphi)$, scaled by (σ/R), for four monodisperse emulsions having radii $R=0.25$ μm (●), 0.37 μm (△), 0.53 μm (■), and 0.74 μm (◇).

fined. However, they are well defined at larger φ, and we plot $G_p'(\varphi)$ for different radii in Fig. 6. The plateau modulus for each emulsion rises many orders of magnitude around $\varphi \approx 0.60$. Emulsions comprised of smaller droplets have distinctly smaller φ at which the onset of the rise occurs. At high φ, where the droplets are strongly compressed, G_p' is larger for smaller droplets. By contrast with Π, the plateau modulus does not diverge as φ approaches unity.

To investigate the role of the interfacial deformation of the droplets on the emulsion elasticity, we scale $G_p'(\varphi)$ by (σ/R), and plot the results in Fig. 7. At high φ, this scaling collapses the data for different droplet sizes. However, at low φ there are large systematic deviations from this scaling. To reconcile these apparently different onset volume fractions, we must account for the electrostatic repulsion between the interfaces of droplets stabilized by ionic surfactants; this alters the φ dependences of G and Π. By using $\varphi_{\rm eff}$ [cf. Eq. (1)] instead of φ, we account for the thin water films stabilizing the charges between the droplets. These thin films will make the apparent packing size of each droplet larger. However, the thickness of the film will be determined by a balance between the screened electrostatic forces between droplets and the deformation of their interfaces. Thus the actual film thickness will be only weakly dependent on droplet size, but will make a relatively larger contribution for the packing of small droplets than for large droplets.

The film thickness itself depends on φ, but in some unknown fashion. Thus we linearly interpolate between a maximum film thickness, $h_{\rm max}$, at low φ, below rcp, where the droplets are not deformed, and a minimum film thickness $h_{\rm min}$, between the facets of the nearly polyhedral droplets at $\varphi_{\rm max}$ near $\varphi \approx 1$. Stable Newton black films of water at a similar electrolyte concentration have been observed with $h_{\rm min} \approx 50$ Å [48]. This is comparable to the calculated Debye length $\lambda_D \approx 30$ Å, for 10-mM SDS solution. Thus we assume that $h_{\rm min}=50$ Å; this makes a larger correction for the smaller droplets. To determine the maximum film thickness, we vary $h_{\rm max}$ until the scaled $G_p'(\varphi_{\rm eff})$ for all droplet sizes collapse onto one universal curve. We find that the film thickness for weak compression which gives the best collapse is $h_{\rm max}=175$ Å, and is the same for all droplet sizes, as shown in Fig. 8. This film thickness agrees with the measured separation between the surfaces of monodisperse ferrofluid emulsion droplets at the same SDS concentration [49], lending credence to its value. Near rcp, the film increases the volume fraction more for smaller droplets, about 5% for $R=0.25$ μm, and only 1% for $R=0.74$ μm.

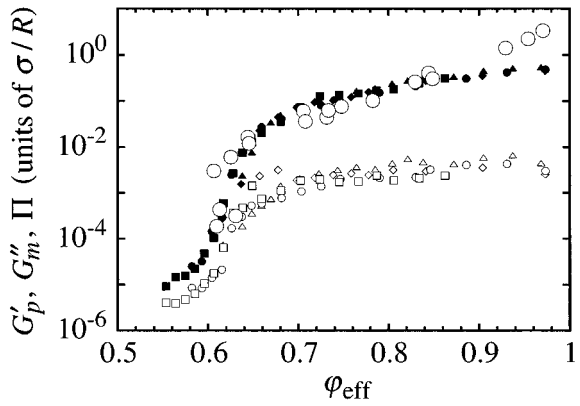

FIG. 8. The scaled plateau storage modulus $G_p'/(\sigma/R)$ (small solid symbols), and the scaled minimum of the loss modulus $G_m''/(\sigma/R)$ (small open symbols), as a function of $\varphi_{\rm eff}$ for monodisperse emulsions having radii $R=0.25$ μm (○), 0.37 μm (△), 0.53 μm (□), and 0.74 μm (◇). The (○) symbols are the measured values of the scaled osmotic pressure $\Pi/(\sigma/R)$. The maximum film thickness has been adjusted to $h_{\rm max}=175$ Å to give the best collapse of $G_p'/(\sigma/R)$.

The onset of a large elastic modulus now occurs near rcp, at $\varphi_{\rm eff} \approx \varphi_c^{\rm rcp}$, as expected. We note that this value is not a

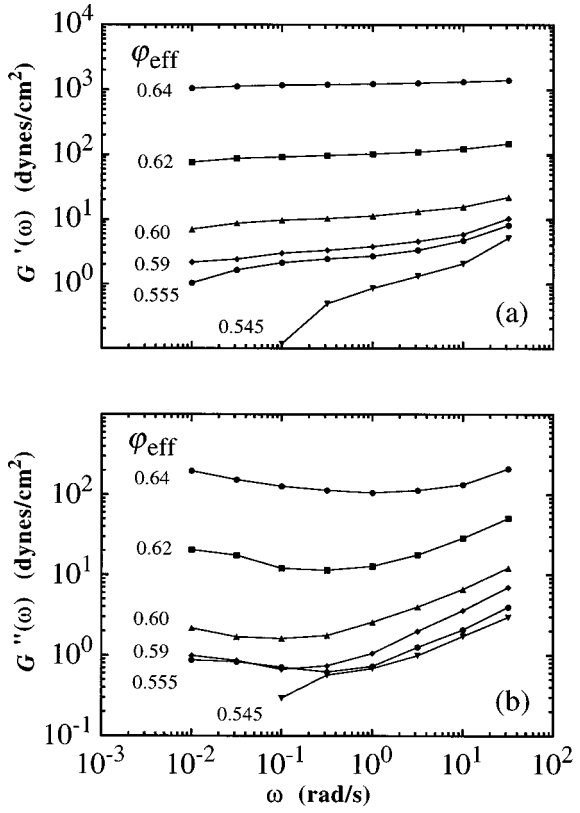

FIG. 9. The frequency dependence of (a) the storage modulus, $G'(\omega)$, and (b) the loss modulus, $G''(\omega)$, for a series of effective volume fractions below the critical packing volume fraction φ_c for $R \approx 0.53$ μm. The lines merely guide the eye.

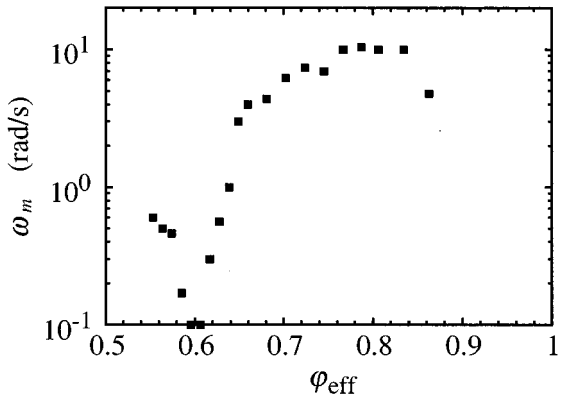

FIG. 10. The effective volume fraction dependence of the frequency where the minimum in the loss modulus occurs, ω_m, for $R=0.53\ \mu$m.

result of our assumption for $h(\varphi)$, but is essentially determined by the measured elastic onset of the largest emulsion, because the 1% adjustment to its φ is very small. The excellent collapse of the data for G_p' and the agreements of $h_{\rm min}$ and $h_{\rm max}$ with independent observations strongly support our use of $\varphi_{\rm eff}$ to account for the electrostatic repulsion between the droplet interfaces.

We also plot the value of the minimum of the loss modulus G_m'' as a function of $\varphi_{\rm eff}$ for each of the droplet sizes in Fig. 8; they also collapse onto a single curve, although the collapse is not as good as for G_p'. At high $\varphi_{\rm eff}$, well above rcp, the elastic modulus is significantly larger than the loss modulus; however, even at lower $\varphi_{\rm eff}$, where the droplets are not deformed, the elastic modulus is still dominant, albeit by not as much. We show more details of this behavior in Fig. 9, where we plot the frequency dependence of both the storage $G'(\omega)$ and the loss $G''(\omega)$ moduli for a series of volume fractions for $R=0.53\ \mu$m. The plateau in G' persists down to $\varphi_{\rm eff}\approx 0.56$ after dropping three orders of magnitude from random close packing; moreover G'' approaches G' as $\varphi_{\rm eff}$ decreases. By contrast, for $\varphi_{\rm eff}\approx 0.55$, $G'(\omega)$ does not exhibit a flat plateau, but instead has a low-frequency dropoff which appears within our measurable frequency range, while $G''(\omega)$ begins to dominate at low frequencies. Measurements at lower $\varphi_{\rm eff}$ are precluded by the stress sensitivity of our rheometer.

The frequency where the minimum in the loss modulus occurs, ω_m, indicates roughly where the contributions from the high- and low-frequency relaxations in the emulsion are equal. Its behavior is plotted as a function of $\varphi_{\rm eff}$ in Fig. 10 for the emulsion having $R=0.53\ \mu$m. Evident is a pronounced dip from $\omega_m\approx 0.5$ rad/s near $\varphi_{\rm eff}=0.57$ to $\omega_m\approx 0.1$ rad/s near $\varphi_{\rm eff}=0.59$, and there is a rapid subsequent rise to nearly a constant value of $\omega_m\approx 10$ rad/s at higher $\varphi_{\rm eff}$. Above this cusp, the frequency of the minimum becomes relatively insensitive to volume fraction, saturating at higher $\varphi_{\rm eff}$.

We have repeated measurements of the frequency spectra, plateau moduli, and minimum in the loss moduli as a function of φ for monodisperse emulsions having a range of oil viscosities: $\eta_o\approx 12$, 235, and 1070 cP. In no case did we observe significant changes in either the magnitudes or frequency dependencies of G' and G''.

C. Discussion

The measured osmotic equation of state is in good agreement with the quasilinear scaling form proposed in Eq. (6). This is shown in Fig. 3 by the solid line, which is a fit to Eq. (5), choosing $\alpha=2$. With this choice, a effective critical value of $\varphi_c=0.60(2)$ is obtained, in reasonable agreement with $\varphi_c^{\rm rcp}$. A similar behavior has been reported for polydisperse emulsions [19], albeit with a considerably larger $\varphi_c\approx 0.72$. This increase in φ_c suggests that polydisperse emulsions can pack more efficiently to higher $\varphi_{\rm eff}$ because smaller droplets can fit in the interstices of larger droplets without deforming. Near $\varphi_{\rm eff}\approx 1$, our data show that Π begins to diverge, with $\Pi\approx\sigma/R$ at $\varphi_{\rm eff}\approx 0.9$, similar to the observed behavior of polydisperse emulsions [19]. This suggests that $\Pi(\varphi_{\rm eff})$ for highly compressed emulsions is relatively insensitive to the polydispersity, with the average droplet size setting the characteristic Laplace pressure scale.

Perhaps the most surprising result comes when we compare the normalized elastic modulus $G_p^{IH}(\varphi)/(\sigma/R)$, with the normalized osmotic pressure $\Pi(\varphi)/(\sigma/R)$. We find that their magnitudes are similar over a range of $\varphi_{\rm eff}$ above φ_c, as shown on a linear plot in Fig. 1. $G_p'(\varphi)$ tracks the osmotic pressure, rising nearly linearly with $\varphi_{\rm eff}$ above the critical volume fraction $\varphi_c\approx 0.64$ corresponding to rcp. The association of this rise with rcp is evidence that the macroscopic rheology is probing the elasticity of the packing of disordered droplets. The similarity between $\Pi(\varphi)$ and $G_p'(\varphi)$ over a large range of φ is reminiscent to the critical-state theory of soil mechanics, where the resistance to shear is proportional to the hydrostatic pressure with a proportionality constant increasing with (soil) packing density [50].

When the droplets are highly compressed, near $\varphi_{\rm eff}\approx 1$, the emulsion's elasticity resembles that of a dry foam and is determined by σ/R. For a disordered monodisperse foam, $G_p'(\varphi)$ is predicted to be $0.55\sigma/R$ [36]. As can be seen in Fig. 8, we find that $G_p'(\varphi)$ approaches $0.6\sigma/R$, in excellent agreement with this prediction. The absence of a divergence of $G_p'(\varphi)$ near $\varphi_{\rm eff}\approx 1$ indicates that volume preserving shear does not cause the local radii of curvature at the droplet's edges and Plateau borders to vanish; instead, the shear merely stretches the interfaces. By contrast, the measured Π does exhibit a pronounced increase in slope as $\varphi_{\rm eff}$ approaches unity. This supports its predicted divergence due to the vanishing radii of curvature as water is squeezed out, although an extensive test of the predicted power law, $\Pi\sim(1-\varphi)^{-1/2}$, is precluded by droplet coalescence.

The existence of a well-defined minimum in $G''(\omega)$ (cf. Fig. 5) at high φ contrasts with the monotonic rise found for a foam [51]. The minimum reflects viscous relaxations at both high and low frequencies. The high-frequency rise in $G''(\omega)$ presumably reflects the increasing importance of the molecular solvent viscosity, while the low-frequency rise reflects glasslike configurational rearrangements of the colloidal droplets. As the droplets become more highly concentrated with increasing $\varphi_{\rm eff}$, they cannot rearrange as easily, so this relaxation is pushed to very low frequencies, permitting the existence of a dominant plateau elasticity. This plateau in $G'(\omega)$ and the corresponding minimum in $G''(\omega)$ have been corroborated by recent dynamic light-scattering

measurements of the viscoelastic moduli of concentrated emulsions [52].

The measured frequency dependencies of $G'(\omega,\varphi)$ and $G''(\omega,\varphi)$ for emulsions below φ_c (see Fig. 9) resemble those of glassy hard-sphere suspensions at similar φ [25]. For hard-sphere suspensions, φ is the thermodynamic variable which plays the role of temperature in a normal liquid-glass transition; as it is raised near the glass-transition volume fraction, $\varphi_g \approx 0.58$, a dominant frequency plateau $G'(\omega)$ and a minimum in $G''(\omega)$ have also been observed. These features are the consequences of the glassy relaxation of the droplet configurations, and the rheological behavior can be described using a model based on MCT [25]. This model also accounts for the frequency plateau $G'(\omega)$ and minimum in $G''(\omega)$. This similarity to hard spheres is reasonable, since the droplets are spherical at these φ. Viscosity measurements for dilute φ at the same surfactant concentration have shown that the surface elasticity of the surfactant prevents coupling of flows outside the droplets to their interior [53]. Above φ_g, a hard-sphere suspension loses its low-frequency relaxation and become nonergodic. This implies an ideal zero-frequency elastic modulus in the rheological model [no drop in G' nor rise in $G''(\omega)$ toward low ω]. However, our emulsion data do show evidence of a low-frequency relaxation even for volume fractions well above φ_g where the droplets are highly compressed. This is reflected by the increase in $G''(\omega)$ as ω decreases. This difference suggests that the deformability of the droplets allows a persistent relaxation for emulsions even above φ_g, unlike hard spheres.

Assuming that this minimum frequency is proportional to the β-scaling frequency in simple mode-coupling theory, which is expected to show a dip (cusp) at the glass transition volume fraction [23], we can identify $\varphi_g \approx 0.59$ for our emulsion from Fig. 10. This is similar to $\varphi_g \approx 0.58$ measured for hard-sphere suspensions [24,25]. These observations are evidence that emulsions first become solids at φ_g, although their elastic moduli are entropic in origin and weak compared to moduli dominated by droplet deformation above φ_c. The rise in $G''(\omega)$ toward low frequencies above the glass transition is indicative of structural relaxations that persist above φ_g; it may be possible to account for $\omega_m \approx 10$ rad/s at these volume fractions by using a modified MCT, which can account for additional relaxation due to the possibility of thermally induced deformations of the droplets.

It is surprising that the (σ/R) scaling for $G_p'(\varphi)$ also produces a reasonable collapse of the data for $G_m''(\varphi)$ (see Fig. 8), since this scaling is based on an elastic mechanism associated with energy storage, not dissipation. This observation suggests that the Laplace pressure also sets the scale for the loss modulus, just as it does for the storage modulus. This is consistent with a proposed model for the loss modulus [37]. As with $G_p'(\varphi)$, the magnitude of $G_m''(\varphi)$ increases dramatically near φ_c where the droplets begin to pack. In the dry foam limit, $\varphi_{\rm eff} \rightarrow 1$, $G_m''(\varphi)$ approaches $4\times10^{-3}\sigma/R$, about two decades lower than $G_p'(\varphi)$. Since the minimum in $G''(\omega)$ cannot be described by the viscosity of Eq. (7) alone, a meaningful comparison with this theoretical model of dissipation is not possible. Instead, our observations suggest that the the Kramers-Kronig relations connecting $G''(\omega)$ to $G'(\omega)$ may lead to an understanding of the scaling of the minima in the loss modulus with volume fraction and droplet size.

The independence of our results on the internal viscosity of the droplets reflects the domination of the surface tension in the deformation of the droplets at our observation frequencies. To estimate the frequency above which this viscosity may be important, we compare the Laplace pressure with the maximum internal viscous stress possible during shear, $\eta_o\gamma\omega \approx \sigma/R$. Solving for the frequency, we find $\omega \approx (\sigma/R)/(\eta_o\gamma)$. For unity strain amplitude, $\sigma = 10$ dyn/cm, and $R = 1$ μm droplets, the frequency for our most viscous droplets ($\eta_o \approx 1000$ cP) would be $\omega \approx 10^4$ s^{-1}, well above our range of mechanical rheometer. This argument agrees with our observations that the behavior is independent of η_o at low frequencies, although it suggests that the spectra at either higher frequencies or for emulsions with much larger internal viscosities may be influenced by η_o.

IV. NUMERICAL STUDIES

A. Model and method

The difference between the theoretical predictions for the φ dependence of the static shear modulus G of ordered emulsions and the experimental data for $G_p'(\varphi)$ leaves us with several unanswered questions. The effects of disorder, the exact form of the potential, the existence of nonaffine relaxation processes all must be investigated in detail. Existing results provided by 2D simulations are not of great relevance, since most of these effects depend strongly on the underlying dimensionality.

The exact deformation of a single droplet under compression has been studied [16] with the help of Brakke's software [54], which triangulates (discretizes) the surfaces to be minimized under a given set of constraints. This procedure is very intensive computationally; thus only relatively small systems can be studied using this approach [17]. The results obtained for the compression of a single droplet, however, provide valuable physical insights on the increase of the droplet surface upon compression. Moreover, the knowledge of the response potential obtained for an individual droplet can in turn be used in a more coarse-grained model which can represent more droplets and thus include the effects of disorder.

A natural candidate for such a coarse-grained model is to represent a collection of N droplets by N pointlike particles confined in a ''bulk'' system obtained by imposing periodic boundary conditions. The resulting system has a reduced number of $3N$ degrees of freedom. While the total interfacial area of an N-droplet emulsion is essentially a function of $3N$ variables, to a good approximation, the interfacial area of an individual droplet can be described by a function of only the respective positions of all its interacting neighbors. A much cruder approximation, which should be valid at very small compression, consists in approximating the droplet's potential by a sum of two-body interactions and neglecting higher-order terms. While high-order interactions are necessary to account for volume conservation effects such as the divergence of the osmotic pressure at high φ, it is not clear how important they are for moderately compressed emulsions.

In an extensive numerical study [16] of the response of a single droplet to compression by various Wigner-Seitz cells,

it was shown that, for moderately compressed emulsions, the interaction potential U can be approximated by a power law,

$$U(\xi)=k'\sigma R^2\xi^{\alpha}, \tag{8}$$

where k' is some constant, ξ is defined as in Eq. (4), and α is a power larger than 2. The striking point of this study is that high-order terms are important since it was demonstrated that α and k' depend on the number of interacting neighbors. A better fit over a wider range of the data was obtained by

$$U(\xi)=k\sigma R^2[(1-\xi)^{-3}-1]^{\alpha}, \tag{9}$$

which has the advantage of being reducible to terms in $(\varphi-\varphi_c)$ for ordered structures. For the sake of comparison, we shall use both potentials in the present study, with $k'=3^{\alpha}k$.

In order to reconcile computational tractability and the inclusion of three-body and higher interactions, we use the following approach for studying disordered structures: we construct disordered systems of hypothetical soft spheres that interact through a two-body, short-range, central-force repulsive pairwise potential represented by a power law [either Eq. (8) or (9)] with a form (coefficient and exponent) depending on the average coordination number of the system. While still mean field in nature, this potential is a definite improvement over simple two-body interaction potentials. Moreover, the anharmonicity of this potential implies that the system will deform nonaffinely, and this model enables us to measure these effects directly.

Under pairwise repulsive potentials, the particles can be thought of as soft compressible spheres, pushing one another and deforming when their separating distance is smaller than the sum of their undeformed radii. The total energy of the system is the sum of all the energy involved in the interacting pairs. The osmotic pressure is obtained from the virial [55].

With the help of this model, we can study the factors influencing the φ dependence of the static shear modulus G, and thus account for our experimental data. For this purpose, we separately investigate the effects of disorder, and the form of the interaction potential on the elastic response.

B. Numerical results and discussion

1. Ordered systems

It is instructive first to investigate the behavior of regular structures of compressible spheres responding to compression with the repulsive potentials introduced in Eqs. (8) and (9). Since ordered structures can be described by a single node, these problems can be solved analytically and, here, the elastic properties of ordered systems are derived for uniform compressions and uniaxial shear deformations. The deformations are always applied along the principal axes of the usual representative unit cells. The details of the calculations are presented in the Appendix.

For all structures, we define the displacement by [generalizing Eq. (4)]

$$\xi=1-r/R, \tag{10}$$

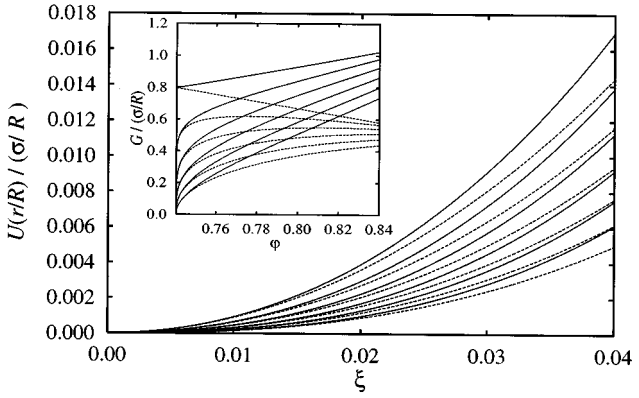

FIG. 11. Two interaction potentials for a maximum displacement corresponding to $\varphi=0.84$. The corresponding static shear modulus of a fcc lattice undergoing a uniaxial strain is shown in the inset. Dashed curves are for Eq. (8) while solid curves are for Eq. (9). Curves are for, top to bottom, $\alpha=2.0$, 2.1, 2.2, 2.3, 2.4, and 2.5.

where R is the undeformed soft sphere radius, and r is half the distance between the centers of two interacting spheres $(r<R)$. By dealing with ordered structures, the shear deformation always leads to the equilibrium (affine) configuration of the system, and, thus, the notion of ''center of the droplet'' still has a meaning.

A springlike potential only takes into account two-body interactions, and thus cannot capture the effects of volume conservation. It is instructive, however, to see how sensitive the shear modulus of ordered structures is to the form of the potential assumed by our hypothetical soft spheres. Figure 11 compares both potentials of Eqs. (8) and (9), with α ranging from 2.0 to 2.5 ($k=1$ has been kept constant in order to spread the curves). In the inset, the static shear modulus of a fcc lattice of hypothetical soft spheres interacting through these potentials and undergoing a uniaxial shear deformation is presented for the same values of α. Numerical surface calculations of the shape of a single droplet uniformly and moderately compressed in a fcc lattice have shown that the excess surface energy per contact can be fit by Eq. (9) with

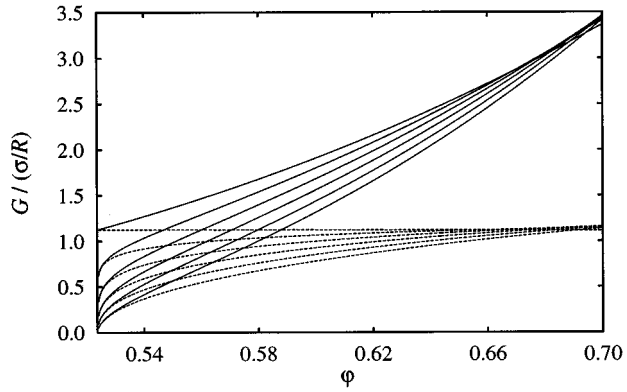

FIG. 12. The static shear modulus of an sc lattice undergoing a uniaxial deformation. The dashed curve are for Eq. (8), while the solid curves are for Eq. (9). Curves are for $\alpha=2.0$, 2.1, 2.2, 2.3, 2.4, and 2.5, from top to bottom.

an exponent $\alpha \approx 2.4$ [16]. The static shear modulus shown in this figure for $\alpha = 2.4$ compares very well with the true uniaxial shear modulus as obtained from numerical calculations of a single droplet uniaxially sheared in a fcc lattice [16].

For anharmonic potentials (i.e., $\alpha > 2$), G exhibits two characteristic features: a sharp onset at φ_c so that $(\partial G/\partial \varphi)|_{\varphi_c}$ diverges, followed by a region where $\partial^2 G/\partial \varphi^2 \lesssim 0$. This is in contrast with experimental data obtained for disordered emulsions, showing a vanishing first derivative at φ_c, followed by an increase of positive curvature. For harmonic potentials ($\alpha = 2$), G exhibits a discontinuity at φ_c [see the analytical form in Eqs. (A4) and (A6)].

Figure 12 shows the same quantities for a sc lattice. Note that for moderate compressions, the true response of a droplet in a sc lattice has an exponent close to 2.2. The static shear modulus obtained from our hypothetical soft spheres interacting with Eq. (9) (and $\alpha = 2.2$) compares very well with the true estimate of G, as obtained from numerical surface calculations [16] or from an expansion at small compression [14].

For a bcc structure, the lattice is unstable under a uniaxial shear along one of its principal axes as such a strain deformation gradually transforms a bcc lattice into an fcc lattice, thus continuously decreasing its energy.

One can also compute the value of the modulus for simple shear strains, as applied along the principal planes (e.g., [100]). The corresponding values of G are only positive for fcc and bcc lattices, since a sc lattice is unstable with respect to this deformation. Calculations of G for simple shear strains give results similar to those obtained for uniaxial deformations, and will therefore not be presented here.

Although a pairwise-potential model can only include radial compressive forces, we demonstrated that it can nevertheless reproduce the qualitative features of the shear moduli of ordered structures, in particular the φ dependence of G.

The calculations of the osmotic pressure are the same for all lattice structures, and are presented in the Appendix. In the vicinity of $\varphi \gtrsim \varphi_c$, both potentials show the same scaling, i.e.,

$$\Pi/(\sigma/R) \approx \frac{k \alpha z_c}{2 a_{\text{cell}}} \left[\left(\frac{\varphi}{\varphi_c} \right) - 1 \right]^{\alpha - 1}, \tag{11}$$

where z_c is the coordination number, and a_{cell} is a lattice specific constant (see the Appendix). The osmotic pressure thus contrasts with G, having a smooth rise $((\partial \Pi/\partial \varphi)|_{\varphi_c} \approx 0)$ at φ_c.

2. Disordered systems

In order to investigate the effects of disorder on the shear modulus, we numerically study disordered systems of N hypothetical soft spheres interacting through the same potentials Eqs. (8) and (9). The systems are cubic and have periodic boundary conditions (PBC's), with N ranging from 1000 to 4913. Smaller systems were also studied, but because of the combined effects of the softness of the potential and PBC's, these systems have a tendency to order spontaneously in fcc at high (osmotic) pressure.

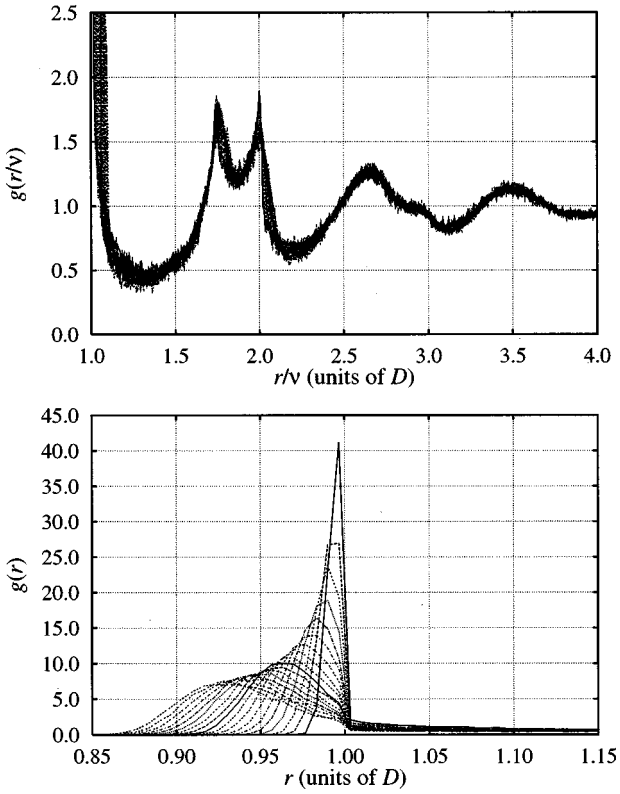

FIG. 13. The radial distribution function of a $N = 4913$ hypothetical soft-sphere system. In (a), the distance has been rescaled by the compression factor $\nu = (\varphi_c/\varphi)^{1/3}$. In (b), the details of $g(r)$ are shown near $r = D$. The curves are for 18 different volume fractions ranging from $\varphi = 0.66$ to 0.85 in steps of ~ 0.01.

The initial configurations are prepared at a volume fraction φ_i by randomly selecting the coordinates of the deformable droplets and then relaxing the system by slowly increasing the potential to its desired value. We find that we must choose $\varphi_i \gtrsim \varphi_c^{\text{rcp}}$ to avoid the slow relaxation observed at random close packing. The systems are then (uniformly) compressed and relaxed in small increments. The relaxation is done by minimizing the energy through a conjugate-gradient algorithm [56] modified to ensure convergence to the closest minimum. At the end of each relaxation, the energy is computed as well as the coordination number and the osmotic pressure. The system is compressed this way until it reaches $\varphi \approx 0.85$, at which value the procedure is reversed, and the shear modulus is computed at each value as φ is decreased.

To investigate the behavior of the packing, in Fig. 13(a) we plot the radial distribution function $g(r)$ of a system of 4913 soft spheres as it is uniformly compressed. The distances are measured in diameter (D) units, and are rescaled by the factor $\nu = (\varphi_c/\varphi)^{1/3} \lesssim 1$. Note how all the curves collapse for large r, showing that there are no large scale rearrangements: contact effects dominate. The radial distribution exhibits the two characteristic peaks of random close packings as discussed by Bernal [57] and Finney [58]: the first one at $r \approx 1.75D$ is related to different local geometries, while the second one is related to colineation of spheres as supported by the sharp drop at $r = 2.0D$ (representing an angle π between three osculatory spheres). These colinea-

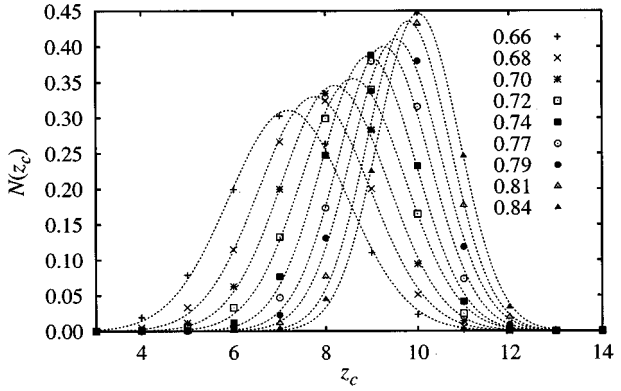

FIG. 14. The probability distribution of the coordination number for the $N=4913$ hypothetical soft sphere system. The curves are fits to Gaussian distributions. The system is uniformly compressed at the volume fractions indicated in the graph.

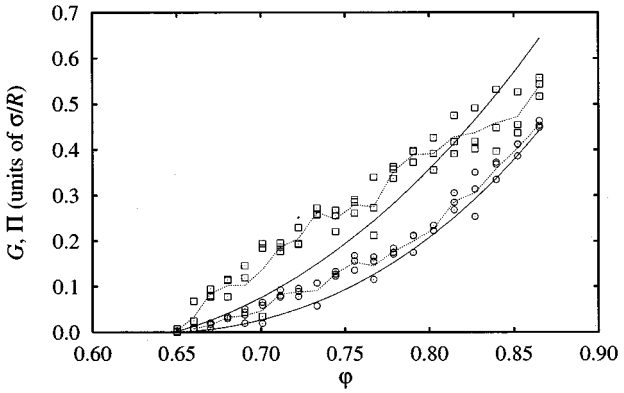

FIG. 15. The static shear modulus of a disordered system undergoing a uniaxial deformation. The potential is as Eq. (9) with $\alpha=2$ (top) and 2.5 (bottom). The symbols represent G (one for a uniaxial strain in each spatial direction) while the solid lines represent Π. (Dotted lines merely guide the eye).

tions, however, are affected by compression, as can be seen from the broadening of the peak: this broadening is due to aligned (angle of π) osculatory triplets that stay aligned and stretched even after compression. This is one indication that the relaxation is nonaffine.

Figure 13(b) shows an expanded view of the contact peak. It is sharp at $\varphi \gtrsim \varphi_c^{\rm rcp}$ and then broadens as the system is compressed, showing that a wide range of interacting contacts is taking place. The sharp cusp at $r=D$ found at moderate φ shows that some spheres can still ''escape'' from interactions with some of their neighbors. The part of the first peak at $r>D$ represents spheres about to touch: any small compression will bring these in contact, thus increasing the coordination number. This presence of such almost osculatory neighbors is also present in packings of hard spheres, making the evaluation of the coordination number rather difficult, and leading to an overestimate in most cases [59]. For soft compressible sphere systems, these ''almost'' neighbors play an important role in the elastic response. This effect is better seen from Fig. 14, which shows the probability distribution of the coordination number for different uniform compressions. This plot exhibits some interesting features of disordered systems. The absence of any node having $z_c=12$ at low compression is striking, showing that rcp has short-range order which favors smaller coordination numbers. The curves are well described by a Gaussian, although there seems to be some systematic skewness at the tails. The mean coordination number increases as the system is compressed, while its distribution appears to be narrower. For an emulsion, the increase of the coordination number plays an important role for two reasons: it increases the number of contacts, and it changes the response of the individual droplets. The first effect is captured by the present model, while the second can be taken care of by modifying the interaction potential as the coordination number changes.

The static shear modulus $G(\varphi)$ is obtained by gradually applying a uniaxial strain in small step increments, relaxing the system (always using the same conjugate-gradient method) at each small shear increment. The size of the shear increments has been tested for reliability: the same results are obtained after halving its value, showing that we are in a regime where G does not depend on the value of the shear strain step increment. We determined that a shear step increment of $\Delta\lambda=10^{-4}$ is an optimal value. For most cases, a maximum strain of $\gamma=0.002$ is sufficient to obtain good numerical data while minimizing the computation: our results demonstrate that with this value, we are in the linear, perturbative regime.

Figure 15 shows the shear modulus and the osmotic pressure of a disordered system of $N=3375$ hypothetical soft spheres interacting with a potential of the form of Eq. (9) with fixed values of $\alpha=2.0$ and 2.5. For both sets of curves, we use $k=1$, so that the amplitude is arbitrary and the two sets should not be directly compared. For $\alpha=2$, G and Π have different slopes at the onset, while for $\alpha=2.5$ the two curves are much closer. The curvature $(d^2G/d^2\varphi)$ is slightly negative for Eq. (9) and $\alpha=2$. Simulations of systems of soft spheres interacting with with Eq. (8) and $\alpha=2$ (i.e., a straight harmonic potential) have a negative curvature that is even more pronounced. The results for Eq. (9) and $\alpha=2.5$ definitely show a positive curvature at the onset, similar to the one observed experimentally. We thus see that the form of the potential has an effect on the qualitative response of the shear modulus of disordered emulsions.

For droplets in ordered lattices, the response to compression depends on the number of neighbors, with an exponent that varies approximately linearly from $\alpha\approx 2.0$ at $z_c=6$ (for sc) to $\alpha\approx 2.4$ at $z_c=12$ (for fcc), when fitting surface calculations results to Eq. (9) [16]. In view of determining the elastic response of disordered systems as precisely as possible, we use the following scheme for the potential: we use Eq. (9) with an exponent that varies according to $\alpha=2+0.4(z_c-6)/6$, and a coefficient $k(z_c)$ obtained from a cubic interpolation scheme between the values obtained for ordered lattices [16]. For a system a $N=1000$ soft spheres, we obtain the curve shown in Fig. 1, where the static shear modulus and the osmotic pressure are compared with the experimental values of the scaled plateau modulus $G_p'(\varphi_{\rm eff})$ and $\Pi(\varphi_{\rm eff})$. For a large range of φ, the agreement between the measurements and simulation results is excellent both in magnitude and overall shape. Such good agreement would not have been obtained without the realistic droplet potential and the disordered droplet structure inherent in the model.

These features of the simulation suggest that the resemblance between $G(\varphi)$ and $\Pi(\varphi)$ found experimentally for emulsions may be fortuitous, resulting from the combined effects of disorder and the particular response of the droplet to compression which can be obtained from purely geometric arguments. However, it may be possible that other heterogeneous dispersions of repulsive elements which interact through more general anharmonic potentials than Eq. (9) may also exhibit the same similarity between $G(\varphi)$ and $\Pi(\varphi)$. Unfortunately, our present knowledge of statistical geometry is not sufficient to either support or rule out such a conjecture.

V. CONCLUSION

Our measurements clearly demonstrate the similarity between the longitudinal $\Pi(\varphi)$, which maintains the static deformation of the droplets, and the transverse $G(\varphi)$ for monodisperse emulsions having a disordered, glassy structure. The monodispersity has enabled us to interpret the strong rise from the entropic to the Laplace scale in terms of packings of monodisperse spheres. In addition, it has allowed us to meaningfully compare the measurements with a three-dimensional model that incorporates both a realistic droplet repulsive potential and a disordered droplet positional structure. The excellent agreement of the simulation based on this model with the experimental results confirm that the origin of this similarity lies in these two essential features.

This central result provides a first insight into the elasticity of disordered packings of identical repulsive elements forced together under an applied osmotic pressure. By contrast to conventional homogeneous solids, in which the moduli of compression and shear are comparable, for disordered heterogeneous solids (e.g., emulsions) the osmotic pressure itself, not the osmotic modulus of compression, may be closer in magnitude to the shear modulus. This similarity may hold for other materials besides emulsions. For instance, our results should be directly applicable to foams comprised of gas bubbles, and they may also provide a guide to the viscoelastic behavior of concentrated microgel beads [60] and multilamellar vesicles [61,62]. The model we have introduced may even provide realistic predictions for their $G(\varphi)$ and $\Pi(\varphi)$, provided an average response of a bead or vesicle to deformation can be calculated.

Despite the success of our model for describing the static elastic modulus and osmotic pressure of compressed emulsions, it cannot predict the full ω dependence of the viscoelastic moduli, since it does not consider dissipative mechanisms. The exact nature of the slow glassy relaxation of the disordered droplet structure, indicated by the rise in $G''(\omega)$ toward small ω, remains obscure for $\varphi > \varphi_g$, especially when the droplets are strongly deformed well above φ_c. In addition to dissipative mechanisms, entropic contributions to $G'(\varphi,\omega)$ and $G''(\varphi,\omega)$ must likewise be included as Π falls well below the Laplace pressure scale, before a meaningful comparison with the experimental data can be made for $\varphi < \varphi_c$. There, the frequency dependence of the viscoelastic moduli exhibits the characteristic rheological features of a colloidal glass: a plateau in $G'(\omega)$, a minimum in $G''(\omega)$, and a frequency associated with minimum $\omega_m(\varphi)$ which exhibits a cusp at the glass transition volume fraction. For undeformed droplets below φ_c, there is a strong similarity between the emulsion's ω-dependent viscoelastic moduli and those of disordered hard spheres, indicating the importance of entropy and the influence of the colloidal phase behavior and glass transition on concentrated emulsion rheology.

This study of the rheology for repulsive monodisperse droplets provides a foundation for comparison with future studies which consider the role of interdroplet attractions and polydispersity. In the case of attractive emulsions, which may form very tenuous solid aggregates or gels of droplets at φ much less than φ_c, the simplicity of our interpretation of the rheology in terms of familiar packings such as rcp may be precluded. In fact, the thermodynamic concept of an osmotic pressure of attractive droplets at dilute φ may be completely different, since the aggregate may not be able to reversibly re-expand once it has been compressed. Likewise, the simple packing interpretation we have used in this study may become much more complicated for polydisperse emulsions. However, by contrast to the past approaches, the effects of polydispersity can now be precisely studied by combining different monodisperse emulsions to generate systematically controllable size distributions. We anticipate that the results of both of these studies will lead to important new results.

ACKNOWLEDGMENTS

We thank Shlomo Alexander, Paul Chaikin, Herman Cummins, Doug Durian, Eric Herbolzheimer, Andrea Liu, David Morse, Tom Witten, and Denis Weaire for many stimulating discussions and suggestions. We are grateful to the *Fonds FCAR du Québec* (M.D.L.), the U.S.-Israel Binational Science Foundation (D.L.), and the NSF (DMR96-31279, D.A.W.) for financial support.

APPENDIX CALCULATION OF G AND Π FOR ORDERED LATTICES

For the sake of demonstration, we derive the shear modulus of a fcc lattice of springlike droplets under a uniaxial strain. To represent the fcc lattice, we choose a unit cell of one node connected to its neighbors by the following 12 vectors:

$$2r'(0,\pm 1,\pm 1)/\sqrt{2},$$
$$2r'(\pm 1,0,\pm 1)/\sqrt{2}, \tag{A1}$$
$$2r'(\pm 1,\pm 1,0)/\sqrt{2},$$

where r' depends on the amount of uniform compression, which is imposed through a factor $\nu=(\varphi_c/\varphi)^{1/3}\leqslant 1$: $r'=\nu R$, where R is the equivalent of the undeformed droplet radius; more correctly in the present context, it is half the range of interaction of our springlike potential. In the present case, $\varphi_c=\varphi_c^{\mathrm{cp}}$ is understood although we use φ_c to simplify the notation. This potential is taken to be

$$U(r)=k\sigma R^2\left[\left(\frac{R}{r}\right)^3-1\right]^{\alpha}, \tag{A2}$$

for $r<R$, and zero otherwise, and k is some constant we define as unity. In order to determine the effect of the exponent α on the shear modulus G, we impose a uniaxial strain on our unit cell: the z direction is stretched by a factor $\lambda=1+\epsilon$, while the perpendicular xy plane is compressed by a factor $\lambda^{-1/2}$. The volume of our unit cell is unchanged by this transformation and remains $2^{5/2}\nu^3R^3$. Applying a uniform compression and a uniaxial shear to the vectors of Eq. (A1), the excess energy density u of our model is

$$u(\lambda,\nu)/(\sigma/R)=\frac{k}{2\sqrt{2}}\ \nu^{-3}\left\{2\left[\left(\frac{\nu}{\sqrt{2}}\ (\lambda^{-1}+\lambda^{2})^{1/2}\right)^{-3}-1\right]^{\alpha}+\left[\left(\frac{\nu}{\sqrt{2}}\ (2\lambda^{-1})^{1/2}\right)^{-3}-1\right]^{\alpha}\right\}. \tag{A3}$$

The shear modulus is obtained for small ϵ (expanding to second order), using $u(\epsilon,\varphi)-u(0,\varphi)=(3/2)G(\varphi)\epsilon^2$ [63],

$$G(\varphi)/(\sigma/R)=\frac{9k\alpha}{16\sqrt{2}}\ \frac{\varphi^2}{\varphi_c^{\alpha+1}}\ (\varphi-\varphi_c)^{\alpha-2}[\varphi(\alpha-2)+\varphi_c]. \tag{A4}$$

One can also define a simpler potential

$$U(r)=k'\sigma R^2\left[1-\frac{r}{R}\right]^{\alpha}, \tag{A5}$$

which is a simple harmonic spring when $\alpha=2$. In this case, we use $k'=3^{\alpha}k$ in order to perform a direct comparison with Eq. (A2). For the same uniaxial strain, the shear modulus of a fcc system of deformable spheres interacting with such a potential is found to be

$$G/(\sigma/R)=\frac{k'\alpha}{16\sqrt{2}}\ \frac{\varphi^{1-\alpha/3}}{(\varphi_c)^{2/3}}\ (\varphi^{1/3}-\varphi_c^{1/3})^{\alpha-2}\times[(\alpha+6)(\varphi_c)^{1/3}-7\varphi^{1/3}]. \tag{A6}$$

A similar procedure is used for determining the shear modulus G of other types of strains and lattices.

The calculation of the osmotic pressure is independent of the lattice structure, since a uniform compression yields the equilibrium configuration. The osmotic pressure is obtained (at $\epsilon=0$) from the energy density by

$$\Pi=\varphi\ \frac{\partial u}{\partial\varphi}-u. \tag{A7}$$

For Eq. (A5), one finds

$$\Pi/(\sigma/R)=\frac{k'\alpha z_c}{6a_{\rm cell}}\left(\frac{\varphi}{\varphi_c}\right)^{2/3}\left[1-\left(\frac{\varphi_c}{\varphi}\right)^{1/3}\right]^{\alpha-1}, \tag{A8}$$

where z_c and φ_c depend on the lattice and $a_{\rm cell}=8$, $32/3^{3/2}$, and $2^{5/2}$ for sc, bcc, and fcc, respectively.

For potential Eq. (A2), one finds a similar form, namely,

$$\Pi/(\sigma/R)=\frac{k\alpha z_c}{2a_{\rm cell}}\ \frac{\varphi^2}{\varphi_c^{1+\alpha}}(\varphi-\varphi_c)^{\alpha-1}. \tag{A9}$$

Note that for a disordered structure the coordination number $z_c(\varphi)$ depends on the volume fraction.

[1] P. Becher, *Emulsions: Theory and Practice* (Reinhold, New York, 1965).
[2] F. Sebba, *Foams and Biliquid Foams—Aphrons* (Wiley, Chichester, 1987).
[3] R. B. Bird, R. C. Armstrong, and O. Hassager, *Dynamics of Polymeric Liquids* (Wiley, New York, 1977).
[4] J. D. Ferry, *Viscoelastic Properties of Polymers* (Wiley, New York, 1980).
[5] P. M. Chaikin and T. Lubensky, *Principles of Condensed Matter Physics* (Cambridge University Press, Cambridge, 1995).
[6] J. Bibette, J. Colloid Interface Sci. **147**, 474 (1991).
[7] T. G. Mason, A. H. Krall, H. Gang, J. Bibette, and D. A. Weitz, in *Encyclopedia of Emulsion Technology*, edited by P. Becher (Marcel Dekker, New York, 1996), Vol. 4, p. 299.
[8] H. M. Princen, J. Colloid Interface Sci. **112**, 427 (1986).
[9] H. M. Princen, J. Colloid Interface Sci. **105**, 150 (1985)
[10] H. M. Princen, Langmuir **3**, 36 (1987). .
[11] H. M. Princen, J. Colloid Interface Sci. **91**, 160 (1983).
[12] H. M. Princen, Langmuir **2**, 519 (1986).
[13] D. C. Morse and T. A. Witten, Europhys. Lett. **22**, 549 (1993).
[14] D. M. A. Buzza and M. E. Cates, Langmuir **10**, 4503 (1994).
[15] D. M. A. Buzza, C.-Y. D. Lu, and M. E. Cates, J. Phys. (France) II **5**, 37 (1995).
[16] M.-D. Lacasse, G. S. Grest, and D. Levine, Phys. Rev. E **54**, 5436 (1996).
[17] A. M. Kraynik and D. A. Reinelt (unpublished).
[18] T. G. Mason and D. A. Weitz, Phys. Rev. Lett. **75**, 2051 (1995).
[19] M.-D. Lacasse, G. S. Grest, D. Levine, T. G. Mason, and D. A. Weitz, Phys. Rev. Lett. **76**, 3448 (1996).
[20] G. D. Scott and D. M. Kilgour, Br. J. Appl. Phys., J. Phys. D **2**, 863 (1969).
[21] J. G. Berryman, Phys. Rev. A **27**, 1053 (1983).
[22] A. Gamba, Nature (London) **256**, 521 (1975).
[23] W. Götze and L. Sjogren, Rep. Prog. Phys. **55**, 241 (1992).
[24] W. van Megen and S. M. Underwood, Phys. Rev. Lett. **70**, 2766 (1993); Phys. Rev. E **49**, 4206 (1994).
[25] T. G. Mason and D. A. Weitz, Phys. Rev. Lett. **75**, 2770 (1995).
[26] J. N. Israelachvili, *Intermolecular and Surface Forces* (Academic, London, 1992).
[27] H. M. Princen, M. P. Aronson, and J. C. Moser, J. Colloid Interface Sci. **75**, 246 (1980).
[28] D. M. A. Buzza and M. E. Cates, Langmuir **9**, 2264 (1993).
[29] K. J. Lissant, in *Emulsion and Emulsion Technology*, edited by K. J. Lissant (Marcel Dekker, New York, 1974), Vol. 1, p. 1.

[30] M. L. McGlashan, *Chemical Thermodynamics* (Academic, New York, 1979).
[31] L. D. Landau and E. M. Lifshitz, *Theory of Elasticity* (Pergamon, Oxford, 1986).
[32] A. M. Kraynik, Annu. Rev. Fluid Mech. **20**, 325 (1988).
[33] F. Bolton and D. Weaire, Phys. Rev. Lett. **65**, 3449 (1990).
[34] S. Hutzler and D. Weaire, J. Phys. Condens. Matter **7**, L657 (1995).
[35] D. Durian, Phys. Rev. Lett. **75**, 4780 (1995); Phys. Rev. E **55**, 1739 (1997).
[36] D. Stamenovic, J. Colloid Interface Sci. **145**, 255 (1991).
[37] A. J. Liu, S. Ramaswamy, T. G. Mason, H. Gang, and D. A. Weitz, Phys. Rev. Lett. **76**, 3017 (1996).
[38] T. G. Mason and D. A. Weitz, Phys. Rev. Lett. **74**, 1250 (1995).
[39] W. Götze and L. Sjogren, Phys. Rev. A **43**, 5442 (1991).
[40] I. M. de Schepper, H. E. Smorenburg, and E. G. D. Cohen, Phys. Rev. Lett. **70**, 2178 (1993).
[41] R. A. Lionberger and W. B. Russel, J. Rheol. **38**, 1885 (1994).
[42] A. J. C. Ladd, J. Phys. Chem. **93**, 3484 (1990).
[43] J. Bibette, Phys. Rev. Lett. **69**, 2439 (1992).
[44] V. A. Parsegian, R. P. Rand, N. L. Fuller, and D. C. Rau, Meth. Enzym. **127**, 400 (1986).
[45] R. W. Whorlow, *Rheological Techniques* (Horwood, Chichester, 1980).
[46] A. Yoshimura, R. K. Prud'homme, H. M. Princen, and A. D. Kiss, J. Rheol. **31**, 699 (1987).
[47] A. S. Yoshimura, and R. K. Prud'homme, Rheol. Acta **26**, 428 (1987).
[48] D. Exerowa, D. Kashchiev, and D. Platikanov, Adv. Colloid Interface Sci. **40**, 201 (1992).
[49] F. L. Calderon, T. Stora, O. M. Monval, P. Poulin, and J. Bibette, Phys. Rev. Lett. **72**, 2959 (1994).
[50] G. Y. Onoda and E. G. Liniger, Phys. Rev. Lett. **64**, 2727 (1990).
[51] S. A. Khan, C. A. Schnepper, and R. C. Armstrong, J. Rheol. **32**, 69 (1988).
[52] T. G. Mason, H. Gang, and D. A. Weitz, J. Opt. Soc. Am. (to be published).
[53] T. G. Mason, J. Bibette, and D. A. Weitz, Adv. Colloid Interface Sci. **179**, 439 (1996).
[54] K. Brakke, Exp. Math. **1**, 141 (1992).
[55] M. P. Allen and D. J. Tildesley, *Computer Simulation of Liquids* (Clarendon, Oxford, 1987).
[56] G. Forsythe, M. Malcolm, and C. Moler, *Computer Methods for Mathematical Computations* (Mir, Moscow, 1980).
[57] J. D. Bernal, Proc. R. Soc. London, Ser. A **280**, 299 (1964).
[58] J. L. Finney, Proc. R. Soc. London, Ser. A **319**, 479 (1970).
[59] J. D. Bernal and J. Mason, Nature (London) **188**, 910 (1960).
[60] E. Bartsch, M. Antonietti, W. Schupp, and H. Sillescu, J. Phys. Chem. **97**, 3950 (1992).
[61] D. Roux, F. Nallet, and O. Diat, Europhys. Lett. **24**, 53 (1993).
[62] P. Panizza, Ph.D. thesis, Université Bordeaux I, 1996.
[63] L. R. G. Treloar, Rep. Prog. Phys. **36**, 755 (1973).